



GRIDSA: femtosecond lifetime measurements with germanium detector arrays

F. C. L. Crespi¹, N. Cieplicka-Oryńczak³, M. Jentsch^{2,a}, F. Kandzia², Y. H. Kim², U. Köster², S. Leoni¹, C. Michelagnoli², S. Ziliani¹

¹ Dipartimento di Fisica dell'Università degli Studi di Milano, INFN Sezione di Milano, Milan 20133, Italy

² Institut Laue–Langevin, 71 Avenue des Martyrs, 38042 Grenoble, France

³ Institute of Nuclear Physics Polish Academy of Sciences, 31342 Kraków, Poland

Received: 5 September 2019 / Accepted: 9 February 2020 / Published online: 21 March 2020
© Società Italiana di Fisica and Springer-Verlag GmbH Germany, part of Springer Nature 2020
Communicated by Calin Alexandru Ur

Abstract We demonstrate the possibility to extract nuclear state femtosecond lifetimes from two-step γ ray cascades measured with a Ge-detector array. The technique is based on measuring the Doppler shift of a γ ray, caused by the recoil of a preceding γ ray emission. Since the two γ rays are populating/de-populating the same state they form a start/stop signal, the delay of which is compared to the slowing down motion of the nucleus within the target material. A multi-detector array combined with digital acquisition electronics in list mode, allows to measure several angular combinations and two-step cascades efficiently and simultaneously within one single experiment. The concept was demonstrated with the FIPPS array for the $^{35}\text{Cl}(n,\gamma)^{36}\text{Cl}$ reaction, where we obtained good agreement with literature values showing the validity of the method.

1 Introduction

Information on nuclear state lifetimes is important to probe our understanding of nuclear structure. They allow assigning absolute transition strengths and therefore are essential for probing predictions of theoretical models. The range of nuclear state lifetimes varies over more than 12 orders of magnitude. Accordingly, many different experimental techniques have been developed and can be classified mainly into direct and indirect methods. By “direct” we refer to techniques in which a nuclear decay is directly measured via a “clock”. A well-known example of such a technique is the so-called fast timing method with LaBr_3 scintillators [1], where a two-step γ -ray cascade provides a start/stop signal and the delay between the two signals yields access to the lifetime

of the intermediate nuclear state. As an “indirect technique”, we refer to methods where the lifetime is extracted via a model from other measured quantities. The Coulomb Excitation technique [2], measuring the transition strength, might be considered as an example.

In the case of direct techniques, the main differentiation comes from the availability of clocks. The above-mentioned fast timing technique uses electronic clocks and relies on fast scintillators and signal processing. It requires a sufficient number of detectors for good statistics and nowadays yields access to lifetimes down to a few picoseconds. The method can be applied to a rather large variety of nuclear reactions since it is rather insensitive to potential Doppler corrections. Another advantage of this technique is the insensitivity to details of the de-excitation scheme (especially unknown feeding) since the choice of the “start”-signal γ ray resets memory of the previous de-excitation history.

For short lifetimes – ranging from a few up to hundreds of picoseconds – also recoil distance techniques [3] are known to provide excellent results. Thus these techniques partially complement the fast timing measurements. They rely on nuclear reactions producing a recoiling excited nucleus. The nucleus travels towards a degrader foil at a variable distance and the energies of the emitted γ rays are measured. From the ratio of Doppler-shifted and unshifted γ rays as a function of the degrader distance, it is possible to extract directly the nuclear lifetime of the de-populated state. The main limitation of this technique comes from the imperfections of the target and degrader foil geometries and the fact that sometimes the level of interest might be strongly fed via transitions passing over higher lying long-lived states.

For lifetimes in the range of a few femtoseconds up to about one picosecond Doppler-shift techniques were successfully applied. Among those techniques, we recall the

^a e-mail: jentsch@ill.fr (corresponding author)

Doppler Shift Attenuation (DSA) [4,5], $(n,n'\gamma)$ [6] and the Gamma Ray Induced Doppler (GRID) [7] broadening techniques. The first two methods rely “similarly as the recoil distance approach” on the bombardment of the target by monoenergetic ions (DSA) or neutrons $(n,n'\gamma)$. In both cases, the target nucleus excitation and the recoil are assumed to occur at the same time. The projectile energy is chosen such that the recoiling nucleus stays within the bulk target material and is slowing down via collisions with the surrounding atoms. Typical recoil energies are in the range of up to a few hundreds of keV, yielding slowing down times of several hundreds of femtoseconds. HPGe-detectors are used to measure a Doppler broadened profile, since the γ rays might be emitted during the recoil motion. The amount of Doppler broadening yields information on lifetimes of de-populated states, which can be extracted by comparing experimental spectra with theoretical profiles obtained from computer simulations of the recoiling atoms. In case of DSA, the results are sometimes limited by unknown feeding to the level of interest and geometrical constraints. In the $(n,n'\gamma)$ technique the constraints of the target ground state spin and parity limit the choice of accessible states. Further, the technique requires most of the time massive samples of isotopically enriched material.

In the GRID-technique, one profits from the extraordinary resolution of the crystal spectrometers GAMS [8]. This allows the measurement of the Doppler broadening due to recoil motion induced by the emission of a γ ray. The Doppler broadening of secondary γ rays in a de-excitation cascade contains information on the lifetime of the de-populated nuclear state. It can be extracted by comparing measured profiles with calculations of the slowing down process based on computer simulations. Due to the low luminosity of the instruments, it is only possible to use them at very intense sources, so far only an in-pile irradiation position at the Institut Laue–Langevin (ILL) research reactor, Grenoble, France, was used. Moreover, it is necessary to deploy massive stable targets (natural composition) and only the strongest cascades may be investigated. Due to the in-pile irradiation, the target material is in most cases unusable after the experiment. For lifetimes below hundred femtoseconds the technique becomes very sensitive to assumptions of the slowing down model. Due to the low luminosity of GAMS, it is impossible to pre-select transition cascades via coincidences. Therefore, the technique is also strongly suffering from uncertainties induced by the unknown feeding, which in many cases is the dominating uncertainty in lifetime measurements.

Obviously, each of the quoted experimental techniques has its advantages and limitations. In this paper we would like to describe a direct technique—the **Gamma Ray Induced Doppler Shift Attenuation (GRIDSA) method**—to measure very short lifetimes in the range of a few up to a few hundreds of femtoseconds by means of an array of HPGe-detectors.

This work is triggered by the fact that such arrays have become a standard tool in many nuclear physics laboratories. This approach aims to compensate some of the weaknesses of the GRID-technique. In particular, the use of a detector array should allow one to investigate samples in the milligram range. Further it will use – similar to the fast timing method – a γ -coincidence technique, which eliminates uncertainties from feeding. The GRIDSA technique could also be applied to more complex decay schemes involving very different decay time scales, i.e. fast γ transitions after a beta decay of long lifetime. As a benchmark system we have chosen to apply the GRIDSA technique to known nuclear states in ^{36}Cl , produced by $^{35}\text{Cl}(n,\gamma)$ -reactions using the thermal neutron beam at the FIPPS Spectrometer [10], [9], a HPGe clover detector array at the ILL.

2 The GRIDSA technique

The GRIDSA technique has been first suggested by Kupryashkin et al. [11] and later experimentally demonstrated in more detail by Kahn et al. [12]. They suggested measuring a two-step γ -ray cascade after thermal neutron capture using coincidences. While the neutron itself with 25 meV kinetic energy is not inducing any significant recoil, the emission of a first primary high-energy γ ray with energy E_{γ_1} gives a recoil to the nucleus of mass M into opposite direction. The recoil velocity v_R is on the order of

$$\frac{v_R}{c} = \frac{E_{\gamma_1}}{Mc^2} \simeq 10^{-5} \dots 10^{-6}. \quad (1)$$

Assuming the emission of a subsequent secondary γ ray with energy E_{γ_2} , the observed energy E is given, in the limit of small velocities, by

$$E = E_{\gamma_2} \left(1 + \frac{v(t)}{c} \cos \theta_{\text{rec}} \right), \quad (2)$$

where θ_{rec} is the angle between the vector of recoil motion of the nucleus and the direction of observation of the γ ray, while $v(t)$ is the time dependent velocity of the recoiling nucleus. The detection of γ_1 defines the direction of the recoil, while a second detector measuring γ_2 in coincidence determines the direction of observation. Assuming the lifetime of the intermediate level to be sufficiently short (compared to slowing down of the recoils), the measured energy E will depend on the angle $\theta = \pi - \theta_{\text{rec}}$ between the directions of view of the two detectors. From Eqs. (1) and (2) it is easily inferable that the variation in energy as a function of θ can be up to a few hundreds of eV. These energy shifts are clearly measurable using HPGe-detectors with optimum resolution. For longer lifetimes and therefore larger delays between the two γ -emissions, the slowing down process will decrease the value $v(t)$. Additionally, with increasing number of atomic

collisions the recoil trajectory is no longer clearly aligned with respect to the axis of observation and the dependence on θ_{rec} is lost.

The first above-mentioned works [11, 12], demonstrated the feasibility of such measurements. However, only simple detection schemes with analog electronics were used, which limited the work to an academic proof of principle. In β decay studies, Egorov et al. [13] demonstrated that energy shifts down to a few tens of eV can be measured with HPGe-detectors provided that sufficient statistics are available. In this experiment, a Si-detector array for β -particle detection was used in coincidence with the HPGe-detector, ensuring granularity and higher efficiency for triggering Doppler shifted γ rays. Modern HPGe-detector arrays, in particular arrays of clovers or γ -ray tracking detectors, combined with digital acquisition electronics providing list mode data collection, allow a more practical application of the GRIDSA technique. The main gain with respect to Refs. [11, 12] is expected to come from higher efficiency allowing to trigger also on weaker two-step cascades, while the higher detection granularity provides measurements at different values of θ .

We consider the energy of secondary γ rays γ_2 measured by detector channel with index j under the condition that the primary γ_1 was detected by detector channel i :

$$E_{ij} = \frac{1}{\tau} \int_0^\infty \exp\left(-\frac{t}{\tau}\right) \int \int E_{\gamma_2} \left(1 - \frac{v(t)}{c} (\mathbf{r}_i, \mathbf{r}_j) \epsilon_i(E_{\gamma_1}, \mathbf{r}_i) \epsilon_j(E_{\gamma_2}, \mathbf{r}_j)\right) d\mathbf{r}_i d\mathbf{r}_j dt. \quad (3)$$

In the first integral the time zero is considered as the moment of detection of γ_1 . The vectors $\mathbf{r}_{i,j}$ denote the directions of the primary and secondary γ ray, linked via the angle $\theta_{ij} = \pi - \theta_{\text{rec}}$. The integration covers all possible vectors linking an assumed point source and the respective detector surface. The lifetime of the intermediate nuclear level is denoted by τ . The functions $\epsilon_{i,j}(E_{\gamma_{1,2}}, \mathbf{r}_{i,j})$ denote the detection efficiencies of the detectors i and j depending on the γ -ray energy and impact vectors $\mathbf{r}_{i,j}$. The function $\epsilon_i(E_\gamma) = \int \epsilon(E_\gamma, \mathbf{r}_i) d\mathbf{r}_i$ is the total photo peak efficiency of the detector i for γ rays with energy E_γ .

We assume for simplicity that the integration over the detector geometry can be replaced by a single detection point, i.e. we assume that all the γ rays in a particular detector are detected in a single point, the position of which is calculated similarly to a center of mass. Thus, the coincident detection of two γ rays in detectors i and j provides well-defined angles θ_{ij} . This assumption simplifies Eq. (3) to

$$E_{ij} = \frac{E_{\gamma_2}}{\tau} \int_0^\infty \exp\left(-\frac{t}{\tau}\right) \left(1 - \frac{v(t)}{c} \cos \theta_{ij}\right) dt. \quad (4)$$

As a further simplification, which will be justified below, we assume that the time dependence of the velocity $v(t)$

due to the slowing down can be approximated by a simple exponential law

$$v(t) = v_R \exp\left(-\frac{t}{T}\right). \quad (5)$$

Here T is the slowing down time, specific to each target material and recoil energy. This allows developing Eq. (4) further to

$$E_{ij} = E_{\gamma_2} \left(1 - \frac{E_{\gamma_1}}{Mc^2} \frac{T}{\tau + T} \cos \theta_{ij}\right). \quad (6)$$

This equation yields a qualitative view on the sensitivity of the GRIDSA technique for measuring nuclear state lifetimes via determining the Doppler-shift $E_{\gamma_2} - E_{ij}$: the functional dependence on lifetime and angle is encoded in the term $\frac{T}{\tau+T} \cos \theta_{ij}$, which is plotted in Fig. 1. As can be seen, for nuclear state lifetimes comparable to the slowing down time there is a pronounced angular dependence. This dependence is vanishing if the ratio of lifetime τ to slowing down time T becomes very small or very large.

The total Doppler shift value scales with $E_{\gamma_2} E_{\gamma_1} / Mc^2$. Let E_C be the total energy of the two-step γ -ray cascade and the energy is shared between the two photons as $E_{\gamma_1} + E_{\gamma_2} = E_C$. Obviously, the measured Doppler shift is maximum in the case $E_{\gamma_2} = 1/2 E_C$ meaning that an equal distribution of energy between first and second γ ray is preferred.

The considerations above were based on two simplifications: on the one hand the detectors have been approximated by a detection point and on the other hand the time dependence of the recoil velocity has been assumed to be exponential. In the following we want to justify the validity of the

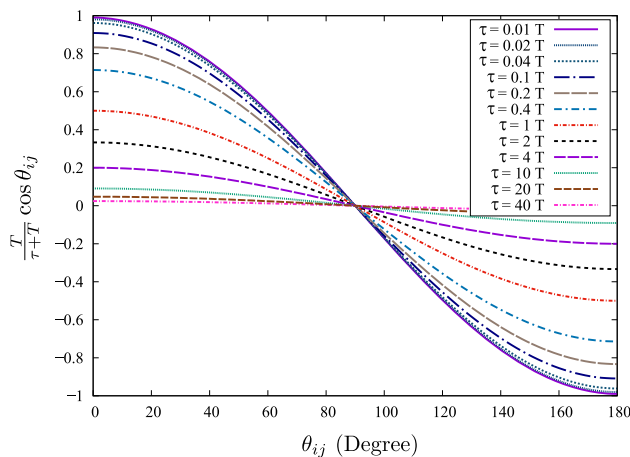


Fig. 1 Dependence of the expected Doppler shift in units of $\frac{T}{\tau+T} \cos \theta_{ij}$ on the angle between the two detectors in which the γ rays were measured. The plots are based on several simplifications (see text) and were done for different ratios of the slowing down time T to lifetime τ . It can be seen that for $\tau \ll T$ and $\tau \gg T$ the curves become almost indistinguishable, which indicates that in these cases the sensitivity with respect to variations of τ is small

two assumptions, which allows us to interpret experimental data using the simple relation of Eq. (6).

The replacement of a complex detector geometry by a single point of detection would require one to carry out a complete mapping of the detector with a collimated point source. This was not carried out for the FIPPS clovers. However, we would refer to experiences with angular correlation experiments carried out with this array. Here, effective point coordinates for a “detection center” for each detector are extracted by comparing experimental data of a two-step transition between states with well-known spin sequence (typically $0^+ \rightarrow 2^+ \rightarrow 0^+$) to a theoretical model based on the coordinates of this detection center. In the particular case of clover detectors (an assembly of four crystals), one could imagine the clover center to be a coordinate origin. The detection point of each detector will be at coordinate (d_x, d_y) , where for symmetry reasons we expect $|d_x| = |d_y| = d$ (see Fig. 2). The point coordinates do not necessarily coincide with the center of each detector crystal and yield specific angular combinations.

Experimentally the values of d were determined for the FIPPS detector array at the ILL by using transitions in ^{116}Sn for which the angular correlations are well known and highly asymmetric. The “effective” center of the detectors was determined by comparing experimental correlation data to known theory and found to be at $d = 1.56$ cm [14] (due to the high symmetry of the FIPPS array a single distance is sufficient to describe the point for all detectors). A plot showing excellent agreement of experimental angular correlation data and theory based on this value of d is shown in Ref. [9]. The determination is based on the analysis of two transitions of 463 keV and 1293 keV, respectively. For the GRIDSA technique, we are more interested in high-energy transitions and therefore it is important to investigate the energy dependence $d(E)$ up to several MeV. We carried out GEANT4 [15] simulations allowing to calculate the energy-dependent efficiency function $\epsilon_i(E_\gamma, r)$ from which we were deducing $d_i(E)$. The results are shown in Fig. 2.

For the transition energies of ^{116}Sn we find approximately the same value of d as it was used for the plot of the experimental data in Ref. [9]. We consider this as an indirect validation of our GEANT4 simulations. In addition, we can conclude that the center is moving mostly in the energy range 0.1–2 MeV, while for higher energies the center position can be considered to be fixed. The knowledge of the detection-point coordinates allows the determination of all angular combinations θ_{ij} .

The second simplification we used to derive Eq. (6) shall be justified by calculating the slowing down process after recoil and comparing the result to an exponential function as in Eq. (5). At the relevant recoil energies of a few hundreds of eV, the slowing down is mainly occurring due to atomic collisions. Electronic excitations and according elec-

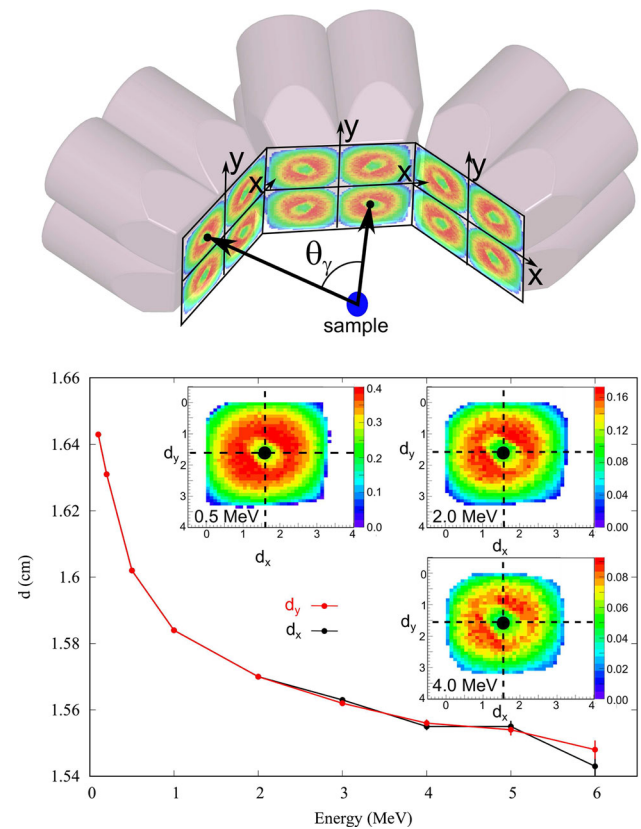


Fig. 2 Schematic visualization of the approach to calculating the detection center coordinates. The contour plots in the upper part indicate the function $\epsilon_i(E_\gamma, r_i)$ obtained by performing GEANT4 [15] simulations and deducing the full photopeak efficiency. The circular modulation of the efficiency is due to the inner hole in each germanium crystal. The diagonal elongation of the circle is due to the position of the source in the center of a clover at a distance of 93 mm but not in the center of an individual crystal. As insert in the lower part we show for three energies how a detection center was calculated (similar to a center of mass). The plot shows the functional dependence of the detection center coordinates as a function of energy. Vertical error bars indicate the statistical error of the simulation. The simulated detection points d_x and d_y are equal within the statistical uncertainty, as expected

tronic stopping power are negligible. This allows us treating the problem in the frame of classical mechanics via molecular dynamics (MD) simulations [16]. The Newtonian equations of motion of several thousand pairwise interacting atoms within a cell with periodic boundary conditions are solved. The recoil motion after emission of a γ ray is obtained by giving one atom the according recoil kick and following its trajectory as a function of time. This process is repeated several times (typically about 1000 recoil events) to sample over all possible recoil directions with sufficient statistics. Such an approach was successfully applied in the past for the interpretation of GRID measurements and the study of atomic motion [17–19]. It is worth noting that the present adopted values of the Evaluated Nuclear Structure Data File (ENSDF) [20] contain data of lifetimes for the 2864, 1959 and 3599

Table 1 Overview of measured transitions feeding and de-populating levels with various lifetimes in ^{36}Cl

Level (keV)	Lifetime adopted values of Ref. [20] (fs)	Populating E_{γ_1} (keV)	De-populating E_{γ_2} (keV)
1601	927 (60)	6978	1601
1959	63 (2)	6620	1959
3599	59 (3)	4980	1131, 3599
2864	21 (1)	5715	2864

keV states in ^{36}Cl , which have been extracted by comparing MD-simulations of a KCl target with GRID data [18].

The benchmark measurements in this work were carried out with NaCl crystalline samples. In the simulation, we had to assume an interaction model for the atoms in NaCl. For interaction energies from thermal up to 5 eV we were using a Buckingham type potential developed by Catlow et al. [21] and deduced mainly from static equilibrium properties of the solid. This potential was splined to a repulsive Screened Coulomb (SC) potential for energies up to several keV. SC potentials are commonly used in computer codes such as SRIM [22,23] to compute the atomic stopping power. In order to illustrate the impact of choosing a particular repulsive potential we used two different models: the ZBL (Ziegler–Biersack–Littmark [22] also used in the slowing down simulation software SRIM [23]) and the so-called krypton–carbon (KrC) potential introduced in Ref. [24], where the KrC is slightly more repulsive.

In Fig. 3 we show the results of such simulations of recoiling ^{36}Cl atoms within a NaCl lattice after emission of the primary γ rays. We focused on four primary γ -ray energies and the according recoils, listed in Table 1. Based on individual event simulation we calculated the average velocity $v(t)$ of Eq. (4). This function was fitted with an exponential function showing reasonable agreement (within the uncertainty of the assumed interaction potential; see the discussion below). The MD-simulations deviate from the smooth exponential behavior by some oscillatory structure. This can be explained by a specific time sequence of collisions in the recoil process due to the crystal structure. From this we deduce that an exponential approximation of the recoil velocity yields a reasonable model.

The impact of changing the SC-potential in the simulations is shown in Fig. 3, top, in the case of the $E_{\gamma_1} = 4.98$ MeV transition. We see that the KrC potential leads to a slightly faster slowing down, which is the result of a more repulsive interaction of the KrC potential. We fitted exponential models to simulation for all transitions and calculated the ratio of extracted slowing down time scales. On average

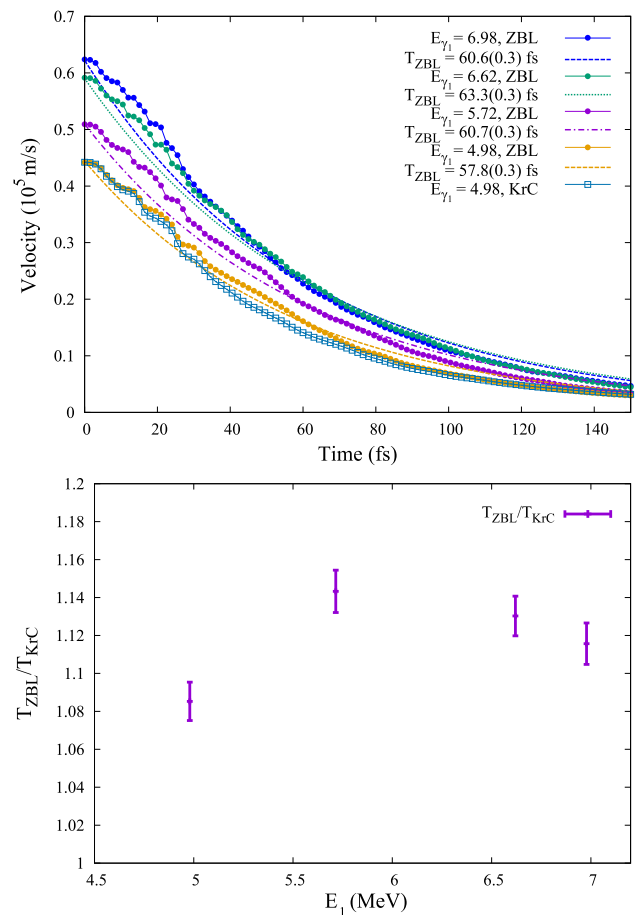


Fig. 3 Upper figure: comparison of molecular dynamics simulation of the recoil motion with an exponential model description of the slowing down. Obviously, a simple exponential model gives a reasonable approximation of the detailed slowing down behavior. The fitted slowing down times vary within $T = 55\text{--}60$ fs. Lower figure: comparison of slowing down times deduced from molecular dynamics simulations using the ZBL and KrC screened Coulomb potentials, respectively. The KrC potential leads on average to about 10% shorter slowing down times

it can be noted that the KrC potential leads to an about 10% shorter slowing down time T than the ZBL simulations (cf. Fig. 3, bottom). Similar aspects have already been discussed in Ref. [18], where variations of up to 30% were obtained. These variations have to be acknowledged as uncertainty of the interaction model and can be transferred onto the error of deduced nuclear state lifetimes.

The discussed models (MD-simulation and exponential slowing down) will be used to extract lifetime data from the experimental GRIDSA data obtained with the FIPPS array. This, together with Eq. (6) shall allow one to have a description of the sensitivity and applicability of the GRIDSA technique.

3 Experimental setup and results

The experiment to test the applicability of the GRIDSA technique was carried out with the FIPPS [9] detector array at the ILL. The array consists of eight HPGe clover detectors arranged in a regular octagon perpendicular to the thermal neutron beam direction. This geometry forms two rings of 16 detector crystals each. The neutron beam is collimated with a set of B₄C and ⁶LiF apertures to a beam diameter of 15 mm and has a capture equivalent flux of up to 10⁸ cm⁻² s⁻¹ neutrons at the target position. The target-to-detector distance is 93 mm.

Data were recorded in triggerless mode, using digital electronics based on V1724 CAEN cards. All cards were synchronized via phase lock to a 100 MHz oscillator. Raw data from the FIPPS detectors were written on disk in list mode. At this stage the data taken from the different detectors were not yet correlated. The correlation was performed in the event building procedure, using information on the time stamp associated to each event. In particular, two detector signals associated to a time difference of less than 500 ns were considered in coincidence. A presorting code was used to perform the energy calibration of the detectors and to produce a ROOT [25] tree with reduced data. The data reduction was done requiring the coincidence of a γ event of energy E_{γ_2} with another γ ray of energy E_{γ_1} . In order to increase statistics, also γ_1 events with reduced energy, associated to the single and double escape peaks due to pair creation, were accepted. For the feeding transitions considered in this paper, being all in the range of 5–7 MeV, this helped to have about 2.5 times larger statistics than gating only on the full energy peak.

The typical energy resolution of the FIPPS HPGe-detectors is found to be 2.5 keV at 1.3 MeV. The applied energy calibrations are of quadratic type and have originally been determined with a ¹⁵²Eu source and a few intense transitions of ³⁶Cl for higher energies. In order to test the impact of increased dispersion we tested different binning of the spectra (within a factor two) and could not find any significant dependence. Throughout the experiment a permanent gain drift of the electronics needed to be corrected for. To do so, the total statistics acquired was subdivided into runs of five minutes allowing a periodic and sufficiently precise calibration check by monitoring the intense 1164 keV and 6111 keV transitions from ³⁶Cl. Based on their variation the energy calibration was corrected for each run. This step was carried out for each Ge crystal channel individually. The effect of this procedure is illustrated in Fig. 4, where the uncorrected and corrected peak positions of one Ge crystal channel are shown for the case of the 2864 keV peak used in the present application of the GRIDSA technique.

Finally, processing the reduced data in the ROOT tree, a matrix E_γ vs. θ is created. This matrix has on the x -axis the angle θ_{ij} between the two detectors i, j that fired in coinci-

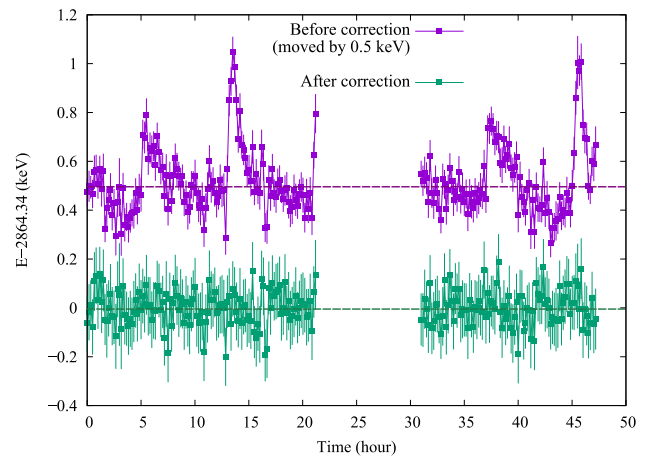


Fig. 4 The effect of calibration monitoring is shown for the 2864 keV transition for a single Ge crystal channel. Two data sets used for the present analysis, interrupted by 10 h, are illustrated. The upper scans (artificially lifted by 0.5 keV) are the uncorrected data assuming the same calibration constants for all times. The lower graphs result from applying a time dependent calibration

dence and on the y -axis the energy E_{γ_2} of the second γ ray, emitted following the one used as a gate for data reduction. The effect of the γ -ray induced Doppler shift can then be observed comparing the γ peaks in the spectra obtained as different y -axis projections of the E_γ vs θ matrix.

The FIPPS clover detectors exhibited a cross talk between neighboring crystals of the same clover during the experiment. When E_{γ_1} and E_{γ_2} were detected in two Ge crystals of the same clover, the energy of the second γ ray was shifted by several hundreds of eV. This process is obviously not related to any physics in the target and unfortunately it is superposing the Doppler-shift signal. Until the phenomenon is sufficiently well understood, we cannot apply any trustable correction to the data. For this reason, in the present data analysis no coincidence combinations of channels within one clover detector were considered. For the same reason we did not use any add-back scheme in the evaluation of our current data. Therefore, the number of coincidence events was significantly reduced. Once the according corrections can be applied the statistical error of the experiment will improve further.

For the benchmark study we chose to focus on the ³⁵Cl(n, γ)³⁶Cl reaction. The targets were composed of NaCl crystalline samples with dimensions 0.2 × 10 × 10 mm³ enclosed in thin Teflon bags. Since the range of recoiling atoms is below 10 nm we can neglect surface effects and all recoil events are assumed to occur in the bulk. The neutron capture cross section (weighted by the isotopic abundance) of 33.0 barn of ³⁵Cl is sufficiently large compared to 0.5 barn of ²³Na yielding an excellent signal-to-noise ratio [26]. A number of nuclear state lifetimes in ³⁶Cl is known to be short, in the range from a few up to 1000 femtoseconds providing a large test ground within one single experiment. Further, the

high chemical reactivity of Cl allows an easy variation of compound chemistry in the future and thereby a variation of the slowing down time.

To demonstrate the applicability of the technique we focused on four states in ^{36}Cl , of which an overview is given in Table 1. The literature values of these states indicate that the potentially achievable sensitivity range of the technique is completely covered.

The choice of a benchmark isotope with a relative high neutron capture cross section does not represent a fundamental limit of the technique. Typically, the mass of the sample is chosen such that the count rate of the individual detector channels is in the order of 5–10 kHz. Therefore, a lower capture cross section of target isotopes may be compensated by a larger target mass. At FIPPS angular correlation experiments—having similar statistical and geometrical constraints—have been successfully carried out with isotopes having capture cross sections down to 0.1 barn. [27]. This represents one of the main advantages of this technique over the GRID-technique with GAMS, where the choice of target mass is restricted: On the one hand the sample has to contain a sufficient number of target isotopes to ensure sufficient intensity. On the other hand targets loaded into the in-pile position of the ILL reactor are limited in mass, volume and thermal resistivity due to self-heating close to the reactor core. In addition, these targets cannot be recuperated after irradiation. Therefore, measurements with exotic materials (isotopically enriched targets, fragile chemical compounds) are not possible with the GRID-technique.

The present data are based on 38 h data acquisition, yielding in total $3.4 \cdot 10^9$ events. In Fig. 5 we show as an illustration the measured Doppler shifts for the 2864 and 1601 keV transitions for detector combinations under $\theta_{ij} = 45^\circ$ and 135° . In the analysis, the energies E_{ij} as a function of the angle θ_{ij} were extracted as barycenter of each peak. The experimental results of this procedure are shown in Fig. 6.

We extracted lifetimes by comparing the MD-simulations with ZBL- and KrC-potentials directly to the data using Eq. (4). In this case, the lifetime error is extracted from the $\chi^2(\tau)$ curve, which yields an asymmetric lifetime error. This can be explained by the fact that an increasing lifetime is associated with smaller shifts. Therefore, the upper limit of the error bar must be larger to achieve the same statistical significance. With an increase of the lifetime value, the asymmetry is more and more pronounced. Additionally to the direct comparison with MD-simulations, we used the exponential slowing down model of Eq. (6). For this purpose individual slowing down times T were extracted as shown in Fig. 3 and then Eq. (6) was fitted to the data. For demonstration purposes we used in these cases an error bar resulting directly from the fit program. It is based on the covariance matrix, calculated by the Marquart–Levenberg algorithm at the minimum of χ^2 . Based on this matrix, the $\chi^2(\tau)$ is approximated by a paraboloid, which

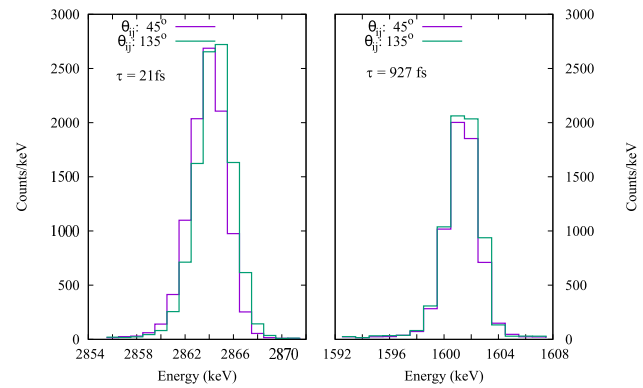


Fig. 5 Spectra showing the 2864 keV (left) and 1601 keV (right) peaks measured for two different coincidence angles θ_{ij} . For the rather short lived 2864 keV state a clearly visible Doppler shift is detected; for the long lived 1601 keV state the shift is almost invisible. The quoted lifetimes are the adopted values of Ref. [20]

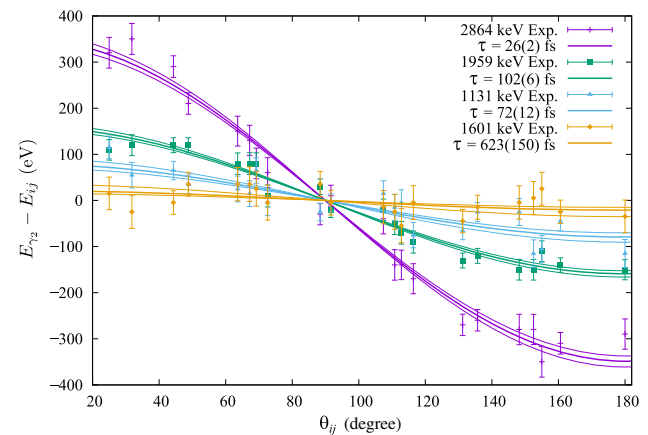


Fig. 6 Experimentally determined values of $E_{ij}(\theta)$ for the four mentioned γ -ray transitions. The data were fitted (thick line) using the expression in Eq. (6), based on the exponential slowing down model. The slowing down times T were determined from MD-simulations with the KrC potential. The thin lines indicate the variation within the error bar

is yielding a symmetric error. We maintain this error bar to demonstrate that the latter approach of error estimate (being more convenient) is in rather good agreement with the former. The results are all summarized in Table 2 and the fits are plotted in Fig. 6. For clarity, we do not plot in Fig. 6 the data from the measurement of the 3599 keV transition due to their large scattering and error bars (see discussion below).

4 Discussion and outlook

In Fig. 7 we present a comparison of the results obtained in the current work with data from other experiments using the GRID and DSA techniques [17, 18, 28–30] contributing to the currently adopted values in the ENSDF data base [20]. We plotted the results of each individual measurement over

Table 2 Overview of measured lifetimes extracted from the GRIDSA data in comparison to the literature values from the Evaluated Nuclear Structure Data Files

Level (keV)	Transition (keV)	τ_{ENSDF} (adopted value [20]) (fs)	τ_{ZBL}		τ_{KrC}	
			MD (fs)	Exp. model (fs)	MD (fs)	Exp. model (fs)
1601	1601	927 (60)	398($^{123}_{79}$)	623 (150)	407($^{125}_{80}$)	559 (135)
1959	1959	63 (2)	107(6_5)	102 (6)	95(9_8)	90 (6)
3599	1131	59 (3)	64($^{10}_8$)	72 (12)	59(8_8)	60 (10)
	3599		68($^{20}_{14}$)	63 (17)	63($^{19}_{13}$)	57 (15)
2864	2864	21 (1)	27(3_2)	26 (2)	24 (2)	23 (1)

For details on the individual models see text. The stated errors of the measured values include only statistical errors

the adopted ENSDF lifetime value of the nuclear state. This allows us to see the scattering of results from each technique and to compare it to the scattering and error bars of the current work.

In general, a rather good agreement of lifetime data extracted from the GRIDSA technique with the literature values of the ENSDF was obtained. A variation of about 10% as a function of the chosen interaction potential used in the MD-simulations can be observed. This is understood as a variation of the slowing down time T when changing from ZBL to the more repulsive interaction of the KrC potential. This effect is mostly pronounced for a lifetime range of 5–200 fs, comparable to the slowing down itself. For longer lifetimes, as the one of the 1601 keV state, it is less significant. Therefore, the purely statistical error quoted in Table 2 should be enlarged by a fraction 0.1–0.2 of the lifetime value to include systematic errors of the slowing down calculations. These uncertainties are also affecting the GRID-technique, as discussed in Ref. [18]. The approximation with an exponential slowing down model does not introduce any significantly larger error in the evaluation and can be used as alternative approach.

For the 1959 keV state the GRIDSA technique yields a longer value than GRID and DSA. Possible explanations could be that the feeding of this state is not clear (42% direct feeding, 30% cascaded feeding and 28% unknown feeding). While DSA and GRID might be sensitive to this, the GRIDSA technique clearly selects a unique feeding scenario. Further, it might be that GRID data of Refs. [17, 18] are biased due to very small MD-simulation cells (a few hundred atoms vs. 10,000 in our case), where for long lifetime simulations the recoiling atom is traversing the simulation cell several times (due to periodic boundary conditions). In order to understand this correctly more measurements and systematic comparisons are required in the future.

The lifetime of the 3599 keV state was measured via two different de-populating transitions: 1131 keV and 3599 keV. According to the discussions of Eq. (6), an optimum sensitivity was expected for $E_{\gamma_2} = E_{\gamma_1}$, a condition which is almost

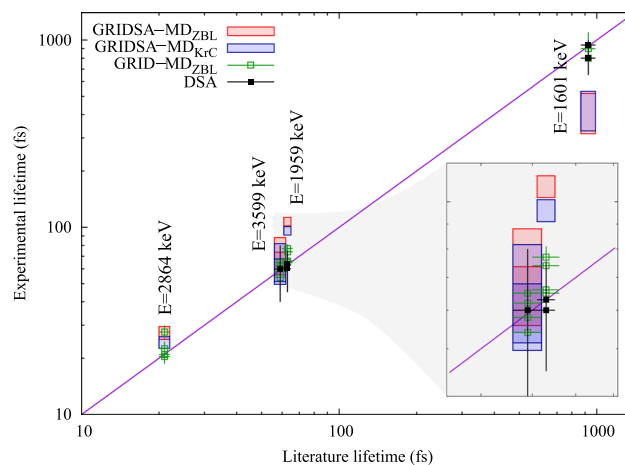


Fig. 7 GRIDSA data compared to the adopted values from Ref. [20]. In general, good agreement over the entire range of sensitivity is obtained. The uncertainty introduced by the slowing down model can be estimated to be about 10% and is well understood

fulfilled for the 3599 keV transition. However, the results in Table 2 show that the lifetime value extracted from the 1131 keV has a smaller error bar, which seems to contradict. This can be explained by statistics arguments: the branching of the 3599 keV transition is six times weaker than that of the 1131 keV transition. Additionally the detection efficiency of the higher energy is lower by a factor 0.4. From this a four times worse statistical sensitivity is expected. This is competing with the enhanced Doppler effect yielding finally an only 1.5 larger statistical uncertainty.

The case of the 3599 keV state can also be used to explore the sensitivity of GRIDSA. The Doppler shift of the 1131 keV transition is roughly three times smaller than the one of the 3599 keV transition. Smaller Doppler shifts could also be caused by longer lifetimes or less fortunate combinations of E_{γ_1}/M due to higher isotope masses or lower E_{γ_1} energies. One conclusion is that GRIDSA could measure comparable lifetimes for masses up to $M \sim 100$ assuming comparable values of E_{γ_1} . Similarly, longer lifetimes up to a few hundred femtoseconds can be measured with the GRIDSA tech-

nique if the recoil velocities are comparable to the example in this work. In all cases sufficient statistics is required and of course all arguments interfere with the performance (resolution, time stability of calibration) of the detection system.

In the current experiment we start to see a substantial deviation (by about a factor of two) from the ENSDF values for a lifetime close to one picosecond. The deviation is not covered by the statistical error bar indicating that systematic effects might affect the experiment. A possible unknown systematic error could be a residual time instability of the gain, which we were not able to remove. This size of Doppler shifts seem to represent the current sensitivity limit the GRIDSA method.

The applicability of the GRIDSA technique is not limited to the (n,γ) reaction. It should be possible to use it for any combination of two subsequent γ rays, provided the nucleus was at rest before the emission of γ_1 . For this purpose it is sufficient that a long-lived nuclear level is populated before emission of γ_1 allowing to reset the “history” of previous recoils, related either to the excitation of the nucleus (via projectiles in accelerators) or to the emission of decay products.

It is important to underline that the strength of the technique lies in the fact that it allows for measuring several lifetimes at the same time. GRID measurements are much more time consuming since they focus on lifetime measurements one by one: For example, the measurement of the four lifetimes in ^{36}Cl with the GRID-technique would require a beam time of about 10 days at the ILL high flux reactor. With the GRIDSA technique at FIPPS, the four lifetimes were measured simultaneously within less than 2 days only. Rather low constraints on the choice of target material and the possibility to recover the target after the experiment are another advantage of the technique over GRID experiments. As such, neutron capture induced femtosecond lifetime experiments with highly enriched or exotic targets become possible at FIPPS. Another strength of the technique is the fact that it removes uncertainties associated with the feeding of the level of interest. Unknown feeding is for many lifetime techniques, in particular for the GRID-technique, one of the major contributions to the final error bar.

The GRIDSA technique does not require any specific modification with respect to a γ -ray spectroscopy setup. It is based purely on a dedicated data evaluation of normal spectroscopic runs and may be applicable to already existing data sets taken with many detector arrays around the world.

Presently used solid-state targets limit the sensitivity of GRIDSA to a few hundreds of fs. This comes essentially from the values of T in the order of a few tens of fs. To extend the method towards longer lifetimes it is necessary to decrease the density of the target material. Therefore, future tests of the technique will include gaseous targets with three orders of magnitude lower density. The flight path of a recoiling atom should be substantially longer than in solid targets, enabling to measure lifetimes up to a few ps.

Data Availability Statement This manuscript has associated data in a data repository. [Authors' comment: The reference to the data is already included in the references of the paper as DOI].

References

1. J.M. Regis, M. Dannhoff, J. Jolie, Nucl. Instrum. Methods A **897**, 38 (2018)
2. P.J. Nolan, J.F. Sharpey-Schafer, Rep. Prog. Phys. **42**, 1 (1979)
3. A. Dewald et al., Prog. Part. Nucl. Phys. **67**, 786 (2012)
4. P. Petkov et al., Nucl. Instrum. Methods A **560**, 564 (2006)
5. T.K. Alexander, J.S. Forster, Adv. Nucl. Phys. **10**, 197 (1978)
6. T. Belgya et al., Nucl. Phys. A **607**, 43 (1996)
7. H.G. Börner, J. Jolie, J. Phys. G **19**, 217 (1993)
8. E.G. Kessler et al., Nucl. Instrum. Methods A **457**, 187 (2001)
9. C. Michelagnoli et al., EPJ Web Conf. **193**, 04009 (2018)
10. <https://doi.org/10.5291/ILL-DATA.3-17-7>
11. V.T. Kupryashkin et al., AN SSSR Ser. Fiz. **53**, 2 (1989)
12. T. Kahn et al., Nucl. Instrum. Methods A **385**, 100 (1997)
13. V. Egorov et al., Nucl. Phys. A **621**, 745 (1997)
14. Private Communication with C. Michelagnoli and J. Jolie
15. S. Agostinelli et al., Nucl. Instrum. Methods A **506**, 250 (2003)
16. M. Meyer, V. Pontikis, Computer simulation in materials science: interatomic potentials. In *Techniques and Applications, Proceedings of ASI* (Kluwer Academic Publishers, Aussois, 1991)
17. S. Ulbig et al., Phys. Lett. B **259**, 29 (1991)
18. A. Kuronen et al., Nucl. Phys. A **549**, 59 (1992)
19. M. Jentschel et al., Nucl. Instrum. Methods B **115**, 446 (1996)
20. <https://www.nndc.bnl.gov/ensdf/>. Accessed 25 Jan 2020
21. C.R.A. Catlow et al., J. Phys. C **10**, 1395 (1977)
22. J.F. Ziegler, J.P. Biersack, U. Littmark, *The Stopping and Range of Ions in Solids* (Pergamon Press, New York, 1985)
23. J.F. Ziegler, J.P. Biersack, M.D. Ziegler, SRIM—the stopping and range of ions in matter (SRIM Co. ISBN 978-0-9654207-1-6. 2008) (2008)
24. W. Wilson et al., Phys. Rev. B **15**, 2458 (1977)
25. <https://root.cern.ch/>. Accessed 25 Jan 2020
26. Information extracted from the NuDat 2 database. <http://www.nndc.bnl.gov/nudat2/>. Accessed 25 Jan 2020
27. N. Cieplicka-Oryńczak et al., Acta Phys. Pol. B **49**, 561 (2018)
28. J.A.J. Hermans et al., Nucl. Phys. A **284**, 307 (1977)
29. A.S. Yousef et al., Phys. Rev. C **8**, 684 (1973)
30. E.K. Warburton, Phys. Rev. C **7**, 1120 (1973)